J. Appl. Comput. Mech., 7(2) (2021) 849-857
DOI: 10.22055/JACM.2020.34992.2534

ISSN: 2383-4536
jacm.scu.ac.ir

Shahid Chamran
University of Ahvaz

Journal of
Applied and Computational Mechanics

Research Paper

Method of Unsteady Hydrodynamic Characteristics Determination in Turbulent Boundary Layer

Vasiliy Shabarov[1], Pavel Kalyasov[2], Vitaliy Shaposhnikov[3], Fedor Peplin[4]

[1] Institute of Informational Technologies, Mechanics and Mathematics, Lobachevsky University of Nizhniy Novgorod, 23 Prospekt Gagarina, Nizhniy Novgorod, 6039506, Russia

[2] Center for hydroacoustics, Institute of Applied Physics of the Russian Academy of Sciences, Ulyanov St, 46, Nizhny Novgorod, 603155, Russia, Email: pkalyasov@mail.ru

[3] Center for hydroacoustics, Institute of Applied Physics of the Russian Academy of Sciences, Ulyanov St, 46, Nizhny Novgorod, 603155, Russia, Email: shaposhnikovva@mail.ru

[4] Institute of Informational Technologies, Mechanics and Mathematics, Lobachevsky University of Nizhniy Novgorod, 23 Prospekt Gagarina, Nizhniy Novgorod, 6039506, Russia, Email: f-peplin@yandex.ru

Received September 11 2020; Revised November 24 2020; Accepted for publication December 30 2020.
Corresponding author: F. Peplin (f-peplin@yandex.ru)

Abstract. This paper presents the method of the turbulent flow simulation. The method may be used to address the computational aeroacoustics (CAA) problems, where the vortex noise's sources have to be determined. This method is an alternative to both large-eddy simulation (LES) methods and stochastic turbulence simulation techniques. The proposed method is more computationally efficient compared to LES and, unlike stochastic approaches, it does not require empirical constants. The simulation according to this method is achieved in two main stages. During the first step the averaged flow's properties are obtained using the RANS simulation. These properties are used for the formulation of the discrete vortex model on the second step. Vortices' intensities are oscillating with amplitudes and frequencies obtained from the RANS simulation with random phase shifts. Turbulent velocity field is then determined as the sum of averaged flow velocities, velocities induced by the pulsing vortices and velocities induced by the trailing vortices (Kelvin circulation theorem). The method is verified by considering the test problem. The developed turbulent boundary layer near the horizontal wall is simulated by means of both the presented method and the LES method. A good agreement between these two methods indicates on the viability of the approach presented in this paper. However, a thorough investigation of the method is still yet to be accomplished.

Keywords: Turbulence, Boundary layer, Vortex, Large Eddy Simulation.

1. Introduction

An accurate determination of the unsteady characteristics of the turbulent flow is essential for many problems in acoustics, aerodynamics, aero- and thermoelasticity. These problems are common in the shipbuilding industry, aerospace engineering and nuclear engineering.

Currently all these problems are addressed mainly by conducting the physical experiments. Often reliable results may be achieved only with the full-scale models, because in the model tests it is very difficult to ensure for all dimensionless numbers to have the same value for the model and for the full-scale construction. For example, in the investigation of the hydroacoustic noise the simultaneous equality of the Reynolds and Mach numbers is impossible to achieve. Another challenge one confronts in physical experiment is an accuracy of flow characteristics measurements.

Mathematical methods aimed to determine unsteady turbulent characteristics are still in the very early stages of their development. Currently there are several approaches to this problem. They are based either on the direct numerical simulation of the fluid motion (DNS, LES, DES) [1, 2] or on the stochastic methods of the turbulent velocity field generation [3, 4].

There are also papers where the method of vortex panels is used to simulate the unsteady flow [5, 6]. Synthetic Turbulence Generator method has been implemented in ANSYS Fluent software. The velocity pulsations' components are determined by means of the vortex method. The vortices are randomly distributed on the shared boundary of RANS and LES domains [7].

A promising new stochastic approach uses the "frozen turbulence" assumption. This assumption represents the velocity and pressure pulsations via randomly generated signal [8]. Such methods are much more computationally efficient compared to the DNS and LES methods. However, in contrast to the CFD approaches they are not universally applicable and require the initial data targeted specifically for each particular problem and not available beforehand (e.g. time and space scales of the turbulent flow). Besides, this approach does not allow to take into account the elastic properties of the solid in a straightforward manner, hence it is not easily applicable to fluid-structure interaction problems. That is why the application of such methods to the real technical problems is challenging.

Published online: January 01 2021

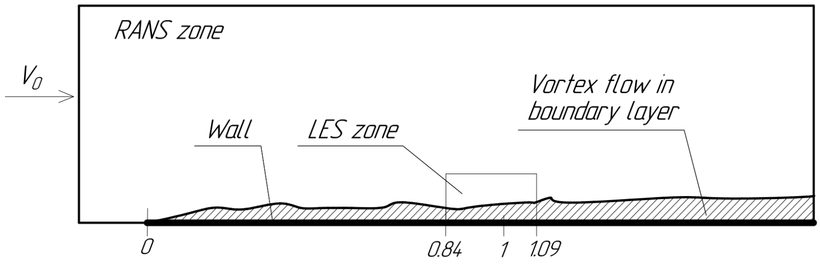

Fig. 1. Boundary layer on the flat wall

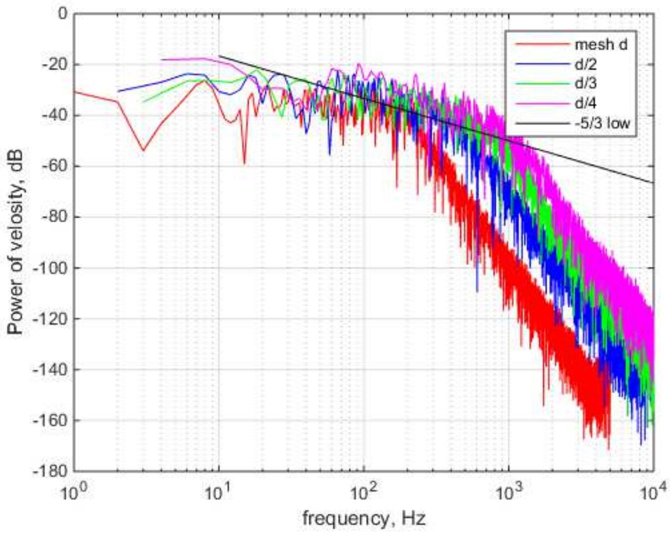

Fig. 2. Velocity pulsation spectrum at the control point of the boundary layer

There are also papers devoted to the multiphase flow simulation. For example, in [9] the modified RANS model is introduced. In this model the term that accounts for the slippage of the dispersed phases relative to the continuous phase is added in the momentum equation. Thus, both turbulent mixture of the particles and their impact on the continues phase are simulated. Significant efforts were devoted to developing turbulence simulation methods for nanomaterials [10-12].

Direct numerical simulation using CFD methods is universal and potentially reliable method. However, such simulations are very computationally expensive. Also, for each particular problem it is required to determine the range of the maximum resolvable frequencies for given grid size. This range of the maximum resolvable frequencies may be limited and not sufficient for the particular problem. Nevertheless, this approach is considered to be the most appropriate for this kind of problems and it is widely used to discover new effects pertinent to the turbulent flow [13].

Let us consider the problem of simulation of the vortex noise generated by a flow near the wing. This problem arises in such areas as aerospace engineering, shipbuilding industry, energy harvesting. In all these cases the reduction of noise is required, which may arise either from flaps, wind generators or propellers. These problems are dealt with in numerous publications, for example, in [14-17]. For small angles of attack the noise is created by an interaction between two turbulent boundary layers behind the trailing edge of the wing.

The crucial part in aerodynamic noise simulation is the determination of the vortex flow's characteristics by means of LES models. To illustrate computational difficulties arising in conducting direct CFD simulations let us apply the LES method to simulate the unsteady turbulent boundary layer near the wall (Fig. 1). The results of this simulation will be used below to verify the proposed method.

According to the ZLES methodology, the computational procedure is divided into two steps. During the first step the averaged characteristics of the flow in the plane setting are determined during the RANS simulation. In this paper the Menter's SST turbulence model is used [18]. This particular model of turbulence was chosen because it is well known and widely used. Besides, this model allows to obtain specific kinetic energy of the turbulence and specific dissipation velocity of the turbulent energy (vortex shedding frequency). This data will be used in the proposed method. The detailed comparison and verification of different turbulence models used in the RANS simulations may be found in [19]. The result of this step is the averaged flow's characteristics. These characteristics coincide with the results of [20] with respect to thickness of the turbulent boundary layer along the shell and velocities in the boundary layer.

During the second step the unsteady flow in the established boundary layer is simulated. Simulation of the three-dimensional flow is performed using the eddy-resolution scheme. The WMLES turbulence model based on the SST Menter's model is used. WMLES model uses RANS simulation near the wall. This reduces required mesh size. In order to minimize mesh size the simulation domain and element size are chosen according to the low bound in the recommendations [21]. Size of the base grid is d = 400 000 elements. Also, additional calculations were conducted with decreased element sizes by 2, 3 or 4 times compared to the base grid. Mesh sizes were: d/2 – 3 million, d/3 – 10 million, d/4 – 30 million.

In Fig. 2 the velocity pulsation spectra at the control point are shown. The control point is located in the boundary layer 0.625 δ from the wall, where δ is the thickness of the boundary layer. Also, the Kolmogorov turbulence law is presented for the isotropic homogeneous turbulence. It is worth noting that increasing of number of elements in the grid allows to simulate larger frequencies of the hydrodynamic pulsations in the boundary layer. This is illustrated in Fig. 3 where the maximum resolvable frequencies are shown for different grid sizes.

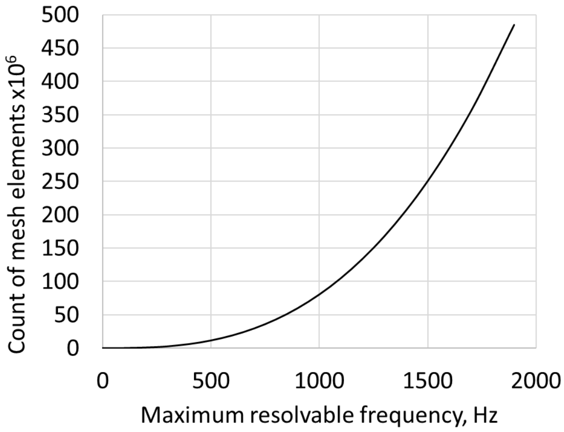

Fig. 3. Dependence of the velocity pulsation's maximum resolvable frequencies in the shell's boundary layer on grid size

Based on these results the required grid sizes were estimated for different values of maximal resolvable frequencies (see Figure 3). According to this data the forecast of [22] may be corrected for the problems in the area of computational acoustics. Specifically, if the required maximal resolvable frequency is 1500 Hz then the required grid size will be at least two orders of magnitude greater compared to the estimation in [22]. Moreover, the number of time steps must be also increased in order to conduct the result processing combined with the averaging procedure. Performing such computations in the foreseeable future is impractical.

In the present paper the method of direct numerical simulation of the vortex fluid motion is introduced. The method combines the vortex method and the RANS simulations. The method uses the Lagrangian approach for the ideal fluid model. The initial data for the vortex system is determined from the results of the RANS simulation. Such an approach resides in the middle ground between the direct numerical simulation and statistical turbulence simulation with respect to required computational resources. Nevertheless, the presented method has an advantage of not requiring time and space scales in contrast to the synthetic turbulence model. As velocity fields obey Euler equations this data is generated automatically.

In what follows the proposed alternative approach to simulate the turbulent boundary layer is proposed (section 2). Then in section 3 this method is applied to the problem of unsteady turbulent boundary layer simulation near the wall considered in this section above.

2. Methodology

The idea of the method is to use the ideal fluid model in order to simulate unsteady hydrodynamic processes. This is achieved by introducing the discrete pulsing vortices-generators which, according to the Kelvin circulation theorem, give rise to the vortex sheds. Amplitudes and frequencies of the vortices-generators are determined by the results of the RANS simulations. Positions and circulations of the free vortices at any given moment in time are calculated from the hydrodynamic theorems. System of vortices creates pulsating contributions to the velocity field. In every moment in time the wall boundary condition on the body surface is satisfied. The result of applying this method are unsteady hydrodynamic forces. These forces may create and sustain high frequency hydroelastic vibrations of different structures and they also may be the sources of the hydroacoustic noise.

Determination of the unsteady hydrodynamic characteristics of the turbulent boundary layer is achieved in three steps. During the first step the model of the viscous fluid is used. The second step is an intermediate step. The goal of this step is to process the results of the previous stage and to prepare the data to the next step. On the third step the model of the ideal fluid is applied.

In what follows the abovementioned steps are discussed in more detail.

2.1 Step 1: Viscous Fluid

During this step the RANS simulations are used to model the turbulent fluid flow near the body. This step is similar to the first step of the aforementioned ZLES method.

The results of this step are: velocity field, specific kinetic energy of the turbulence, specific dissipation velocity of the turbulent energy (vortex shedding frequency) in the centers of the control volumes.

2.2 Step 2: Viscous Fluid (preparation of the data to step 3)

The mesh is created during this step. At this early stage of the method's development the same mesh that was used for the RANS simulation is employed. In the center of each control volume of the domain discrete vortices are placed. Circulation of each vortex changes with time according to the following formula:

$$\Gamma_{pij}(t) = \Gamma^0_{pij} \sin(f_{ij} t + \varepsilon_{ij})$$

where Γ^0_{pij} – amplitude of the vortex-generator's intensity for the control volume ij, ε_{ij}– random numbers uniformly distributed in the interval $[0,2\pi]$, f_{ij}– frequency of the vortex-generator's pulsation in the ij control volume determined via RANS simulations and equals to the turbulent eddy frequency. Note that since the specific turbulent energy in RANS is a constant, velocity of dissipation is equal to velocity of vortex generation.

Amplitudes of the discrete vortices-generators Γ^0_{pij} are determined from the values of the turbulent kinetic energy in the centers of the control volumes. In the plane setting for determination of circulation amplitudes the system of MN nonlinear equations with MN unknown amplitude values of vortices-generators intensities Γ^0_{pij} has to be solved (M, N are numbers of elements over x and y directions respectively).

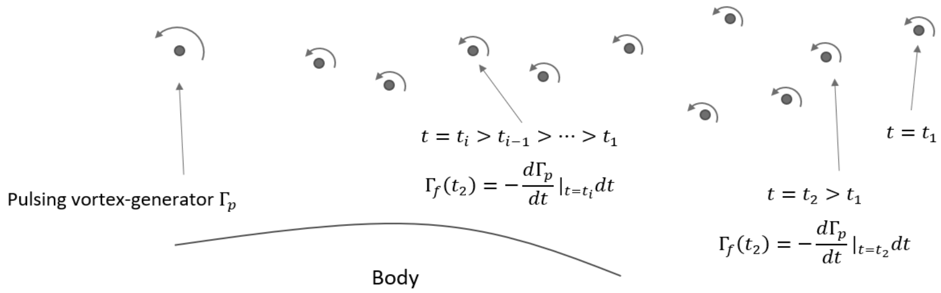

Fig. 4. The pulsating vortex-generator and the vortex shed

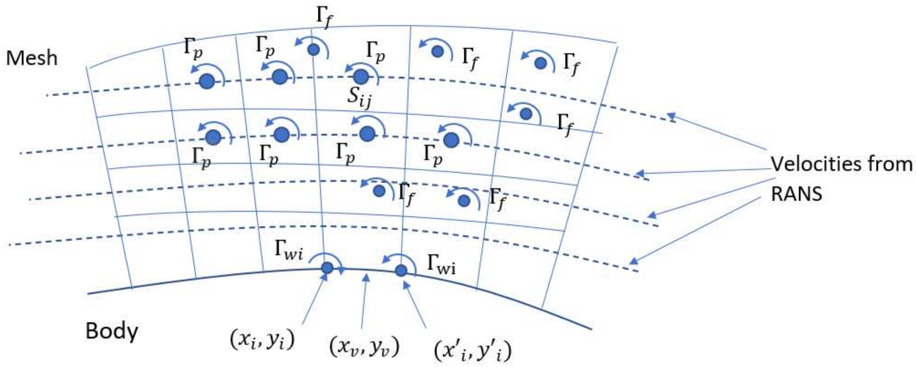

Fig. 5. The wall boundary condition

$$\left(\sum_{\substack{k=1\\k\neq i}}^{M}\sum_{\substack{p=1\\p\neq j}}^{N}\frac{1}{2\pi}\frac{\Gamma^{0}_{p\;kp}(y_{ij}-y_{kp})}{(x_{ij}-x_{kp})^2+(y_{ij}-y_{kp})^2}\right)^2+\left(\sum_{\substack{k=1\\k\neq i}}^{M}\sum_{\substack{p=1\\p\neq j}}^{N}\frac{1}{2\pi}\frac{\Gamma^{0}_{p\;kp}(x_{ij}-x_{kp})}{(x_{ij}-x_{kp})^2+(y_{ij}-y_{kp})^2}\right)^2=2k_{ij} \quad (1)$$

where $i,k=\overline{1,M}$, $j,p=\overline{1,N}$, x_{ij}, y_{ij} -coordinates of control volume's center, k_{ij} - specific turbulent kinetic energy.

After solving system (1) MN random phase shifts ε_{ij} are generated. These numbers are uniformly distributed over the interval $[0,2\pi]$.

2.3 Step 3: Ideal Fluid

As circulations of vortices-generators change according to the harmonic law, each vortex-generator creates a shed of free vortices. According to the Kelvin circulation theorem every pulsing vortex-generator with circulation $\Gamma_p(t)$ gives rise to the free vortex shed with circulations (Fig. 4)

$$\Gamma_f(t^*)=-\frac{d\Gamma_p}{dt}(t=t^*)\Delta t$$

Pulsing vortices-generators are fixed in space while free vortices created by them move with velocities equal to the sums of:

a) velocities in the domain, determined from the results of the preliminary RANS simulations;

b) velocities, induced in instantaneous locations of free vortices by all pulsing vortices-generators and all the rest free vortices (excluding the one being examined);

c) velocities induced by the vortices located on the body's surface. These vortices are needed to satisfy the wall boundary conditions.

Since on the step 3 the ideal fluid model is used the only boundary condition that is imposed on the body surface is the requirement that the normal velocity should vanish.

The body boundary is divided into K elements. Since the main contribution to the forces caused by the vortices-generators and free vortices on the surface elements is due to the unsteady hydrodynamic processes with high values of Strouhal number the flow over each element is assumed to be vortex-free. Hence on every surface element there are discrete vortices with the same circulation but with different signs (see Fig. 5). The wall boundary condition is satisfied in the centers of the boundary elements. These conditions lead to the following system of nonlinear equations with unknown circulations Γ_{wi}

$$\sum_{i=1}^{K}(V_n(\Gamma_{wi},x_i,y_i)|_{x_\nu,y_\nu}+V_n(-\Gamma_{wi},x_i',y_i')|_{x_\nu,y_\nu})=-\sum_{i=1}^{M}\sum_{j=1}^{N}V_n\Gamma_{p\;ij}|_{x_\nu,y_\nu}-\sum_{\substack{Over\ \ all\\ free\ \ vortices}}V_n\Gamma_f|_{x_\nu,y_\nu},\nu=1...K \quad (2)$$

After solving system (2) it becomes possible to obtain the pulsing hydrodynamic pressure on the body's surface according to the following equation:

$$p=-\rho\frac{d\Gamma}{dt}$$

Or, in discrete form:

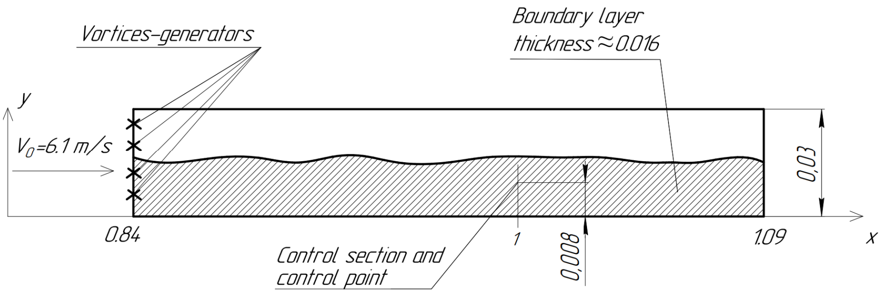

Fig. 6. The simulation domain

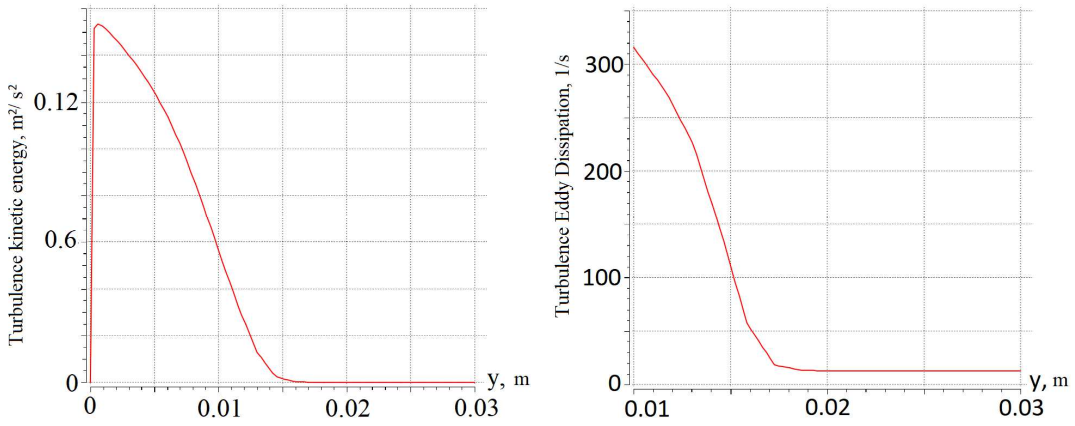

Fig. 7. Turbulence kinetic energy (left) and turbulence eddy dissipation rate (right) at the inlet boundary

$$p(x_i, y_i, t^*) = -\rho \frac{1}{\Delta t}(\Gamma'_{i-1}(t^*) - \Gamma'_{i-1}(t^* - \Delta t) + \Gamma_i(t^*) - \Gamma_i(t^* - \Delta t))$$

$$p(x_i, y_i, t^*) = -\rho \frac{1}{\Delta t}(\Gamma'_i(t^*) - \Gamma'_i(t^* - \Delta t) + \Gamma_{i+1}(t^*) - \Gamma_{i+1}(t^* - \Delta t))$$

It is worth noting that the averaging of the solution for large lengths of the vortex sheds leads to the results very close to those obtained by the RANS simulations with respect to velocity and pressure pulsations, turbulent kinetic energy, turbulent energy dissipation rate and velocity distribution in the boundary layer. From this point of view the presented method is consistent with RANS methodology.

3. Application of the Proposed Method

Let us apply the described method to the problem discussed in the first part of the paper. This problem allows to use the simplified boundary conditions in order to concentrate the efforts on the general idea of the method.

The problem domain is shown in Fig. 6. Size of the domain is the same as for the LES simulation considered above.

The numerical scheme is as follows. In the inlet there are 10 vortices-generators placed vertically. Amplitudes and frequencies of the vortices-generators' intensities are calculated from the RANS simulations' results as follows:

$$\Gamma_{pi}(\mathbf{r}, t) = C\sqrt{K(\mathbf{r})}\sin(f(\mathbf{r})t + \varphi) \tag{3}$$

where K –turbulence kinetic energy, f – turbulence eddy dissipation rate, φ – random phase in the interval [0, 2π]. Quantities K and f are determined from the results of the RANS simulations and depend on the spatial coordinates. Distributions of these quantities at the inlet (x=0.84) are shown in Fig. 7. Constant C = 0.01 is chosen to ensure maximum amplitudes of the velocity pulsations to be the same for the RANS and LES simulations. In general case this constant depends on the discretization parameters and computational radius of the vortex in the model. Vortices-generator are similar to the initial conditions. Characteristics of the vortices-generators are determined exclusively from RANS simulations.

Each vortex-generator creates a vortex shed. At the location of the vortex-generator free vortices are placed with intensities:

$$\Gamma_{f\,ik} = -\frac{d\Gamma_{pi}}{dt}(t = t^*)\Delta t = C\sqrt{K_i} f_i \cos(f_i t_k + \varphi_i)\Delta t \tag{4}$$

where index i denotes that the free vortex belongs to the shed of the i-th vortex-generator, index k determines which group of the free vortices in the time domain this particular free vortex belongs to, t_k is the current moment in time, $\Delta t = \Delta n \cdot dt$ – free vortex generation time step, dt is the time step and Δn is the free vortex generation step. In the present simulation dt is 0.1 ms, total number of iterations is 5000 and Δn = 10. The value of Δn is chosen to preserve the equal distance between the vortices-generators (in the vertical direction) and the free vortices moving in the averaged velocity field. All these parameters characterize discretization scheme. Their impact on the results should be studied separately.

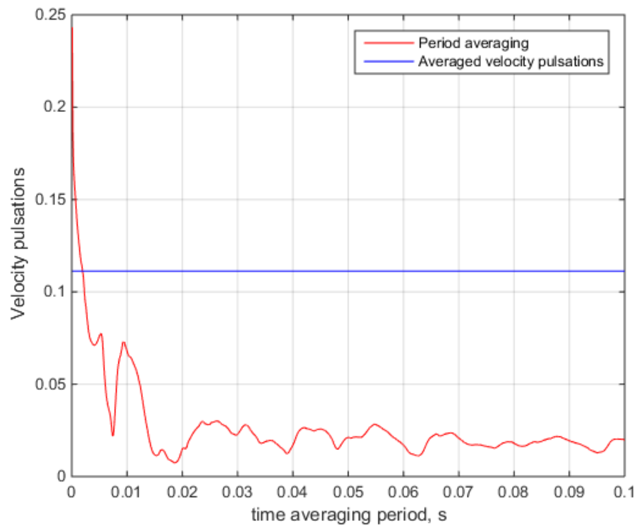

Fig. 8. Averaged velocity pulsations

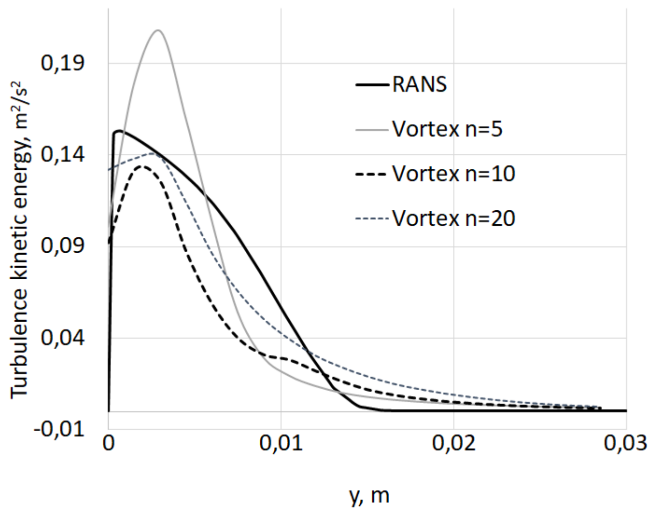

Fig. 9. Kinetic energy in the control section.

The velocity field on every timestep is determined according to the formula

$$\mathbf{V}(\mathbf{r},t)=\mathbf{V}_{RANS}(\mathbf{r})+\sum_{i=1}^{n}\frac{\Gamma_{pi}(t)}{2\pi\,|\,\mathbf{r}-\mathbf{r}_i\,|}\mathbf{e}_i(\mathbf{r})+\sum_{i=1}^{n}\sum_{k=1}^{m}\frac{\Gamma_{fik}(t)}{2\pi\,|\,\mathbf{r}-\mathbf{r}_{ik}(t)\,|}\mathbf{e}_{ik}(\mathbf{r})\;, \tag{5}$$

where $\mathbf{V}_{RANS}$ is the averaged velocity, obtained from the RANS simulations, $\mathbf{r}_i$ and $\mathbf{r}_{ik}$ are radius vectors of vortices-generators and free vortices respectively, e_i, e_{ik} – unit vectors determining velocity directions induced by vortices-generators and free vortices respectively. According to the definition of the vortex, vectors e_i and e_{ik} are tangent to the circles with centers at the vortices' positions. Vortices-generators' positions do not change in time, but their intensities vary according to equation (3). Contrary to the vortices-generators, the free-vortices' spatial positions change, but their intensities remain constant. Spatial position of each free vortex obeys the following law:

$$\mathbf{r}_{ik}(t+dt)=\mathbf{r}_{ik}(t)+\mathbf{V}(\mathbf{r},t)dt\;, \tag{6}$$

Boundary conditions are set as follows. On the rigid wall the no-slip boundary condition is met exactly due to the fact that all the vortices are mirrored relative to the wall with the change of intensities' signs. This approach is applicable only for that particular kind of problem. Generally, when there is no symmetry the algorithm described above has to be implemented. This work is yet to be done. All other faces are free from any boundary conditions. If the vortex leaves the domain it is excluded from the computations. Since the longitudinal component of the averaged velocity is large compared to the pulsation near the inlet, there is no transition of the vortices through this boundary. The upper boundary is outside of the active vortex flow and upper vortices' velocities are determined mainly by averaged velocities from the RANS computations, parallel to the boundary. There are no more than 1% of the vortices leaving the domain through the upper boundary. Excluding the vortices from the computations when they leave the right (downstream) boundary changes the structure of the flow. It is assumed that the outlet boundary lies far away off the control point and the control section, hence the impact of the excluded vortices is negligible compared to vortices located in the vicinity of the control point. In general case, the influence of domain's size has to be investigated for each particular problem separately as it is usually done for the traditional CFD simulations.

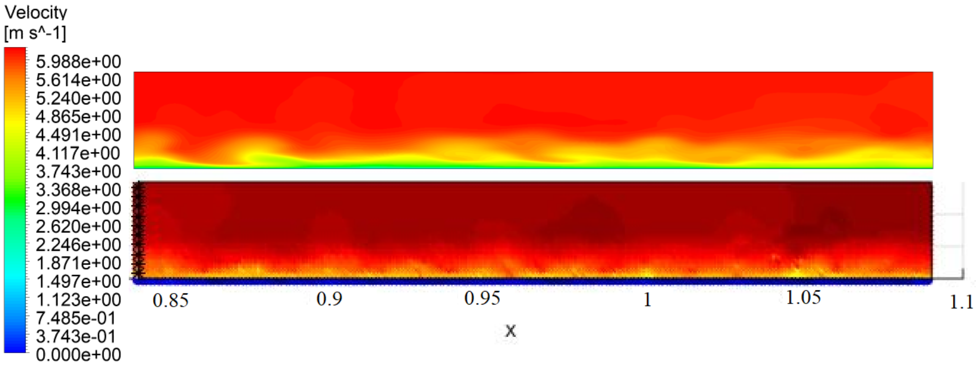

Fig. 10. Instantaneous velocity field for «LES 3D» (in cross section) (top) and «Vortex 2D» (bottom)

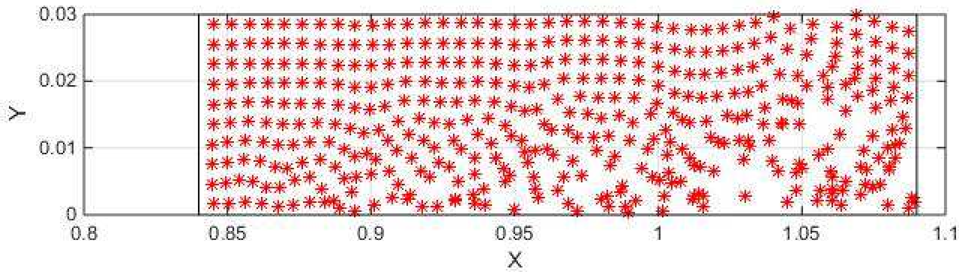

Fig. 11. Instantaneous positions of free vortices

For the specified (basic) parameters of the discretization It took 400 iterations to completely fill the domain with free vortices. After that their quantity remains approximately 430.

As the result of the simulations the unsteady velocity field has been obtained in the entire domain. The analysis is based on the comparison between the turbulence characteristics obtained by the proposed method with the RANS and LES simulations used before. The parameters that have been studied are kinetic energy, turbulence spectra and velocity pulsations spatial correlation. Following conclusions can be drawn from the results.

1. Let us compare the results of the averaged characteristics with the results of the RANS simulation. Velocity pulsations at a point, induced by vortices, are getting smaller with an increase of an averaging period. Nevertheless, they do not vanish completely, but become constant, approximately 10-15% from their average value (Fig. 8). This should be investigated separately. However, the averaged pulsation velocity is only 0.2–0.3% of the averaged flow velocity so it is sufficiently close to zero.

2. The kinetic energy in the control section is distributed similarly according to the RANS simulations and the vortex method (see Fig. 9). In Fig. 9 quantity n denotes number of the vortices-generators in the model. Note that the kinetic energy is an independent variable in RANS. In the vortex model the kinetic energy is calculated from the velocity pulsations field according to the following formula:

$$K = \frac{1}{N}\sum_{j=1}^{N}({u'}_j^2 + {v'}_j^2)$$

where N is the number of timesteps.

3. The comparison of unsteady turbulent characteristics obtained by the presented method and by 3D LES simulation.

In Fig. 10 the velocity fields at some fixed moment in time obtained by means of the LES simulation and the presented method are shown.

Instantaneous positions of free vortices are shown in Fig. 11. The vortices are mixed downwash in the region of large kinetic energy (large circulation). This effect causes decrease of the velocities compared to the averaged velocities obtained by RANS; this leads to the increase in kinetic energy at the boundary layer downstream. Hence the vortex model describes physical processes similar to the turbulence model in RANS simulations.

In Fig. 12 the spectrum of velocity pulsations is shown. The sharp decrease of spectrum obtained from LES simulation is related to the rough (for these frequencies) grid. Given the results of the LES simulations it may be observed that the vortex model describes beginning of the inertial subrange interval of turbulent flow. The vortex simulation allows to obtain all frequencies from this interval. The simulation by means of the vortex method took only 15 minutes (without parallelization) compared to 24 hours for LES simulation (with parallelization in 4 threads).

Another parameter which is used to verify the developed method with LES is the spatial turbulence scale. In Fig. 13 and 14, the spatial correlation of the vertical velocities at the control point in downstream direction and normal to the surface is shown. These results are in good agreement with these two methods in downstream direction. In direction normal to surface there is a discrepancy between two methods which may be explained as follows. Far from the surface the correlation calculated by LES method decreases sharply. This is related to the wall boundary condition on the upper boundary of the domain. Near the wall the disagreement may be attributed to inaccuracy of the vortex model related to the absence of the slipping boundary condition on the surface of the shell. This should be investigated more closely.

4. The influence of the spatial discretization on the results was investigated. In order to reduce the number of discretization parameters the following scheme was used. Number of vortices-generators and free vortices generation step were changing while the ratio of the distance between free vortices to the free vortices' generation step was kept constant. The simulations with 5, 10 and 15 vortices-generators were considered, while the free vortices were generated every 20, 10 and 5 iterations, respectively. The results are in Fig. 9, 12, 13 and 14. According to this data the discretization parameters cause moderate effect on the simulation results.

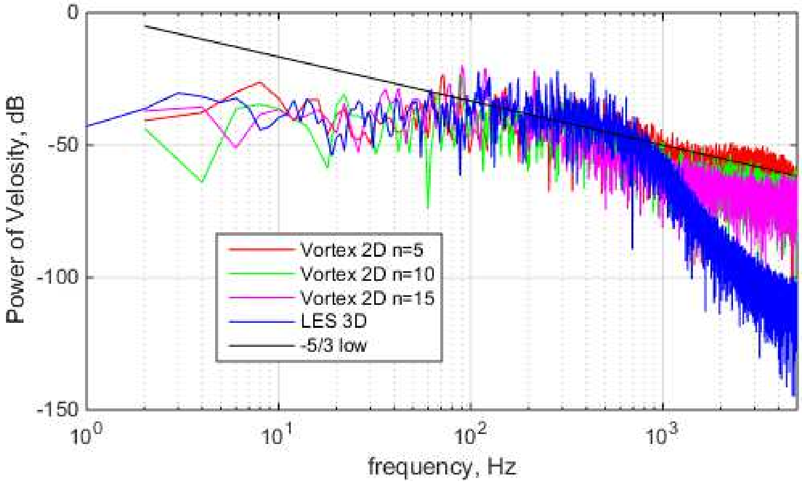

Fig. 12. Spectrum of the velocity absolute value at the control point for «LES 3D» и «Vortex 2D» simulations

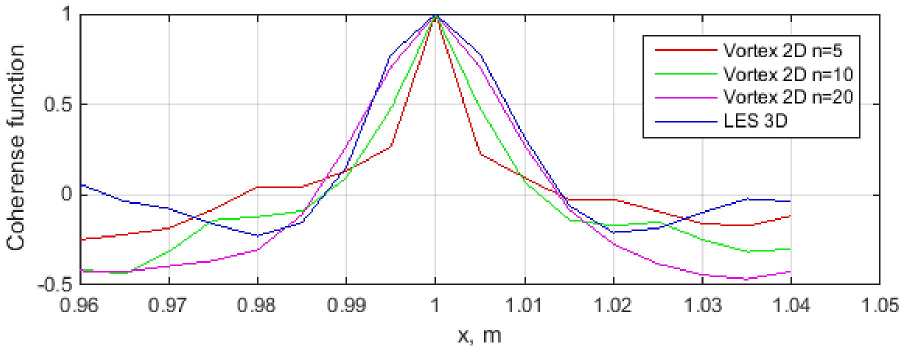

Fig. 13. Correlation of vertical velocities in the downwash direction

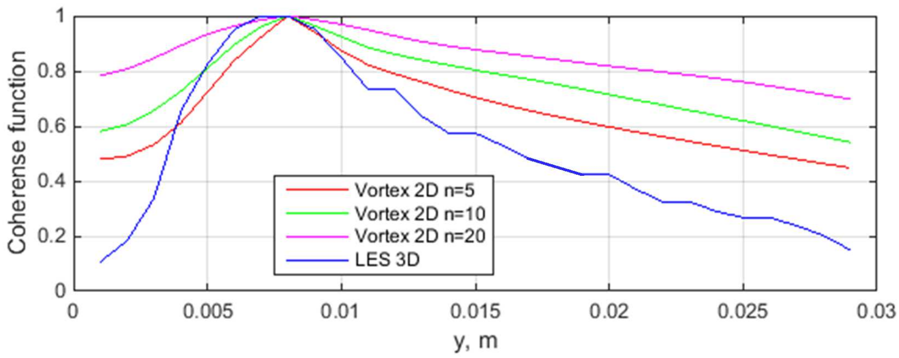

Fig. 14. Correlation of vertical velocities in the direction normal to the wall

Generally, the application of the LES method and the developed method to the particular problem shows good agreement between these two methods. This indicates on the viability of the presented approach and suggests that further investigation is worth the efforts.

4. Conclusion

In this paper the method for determination the velocity and pressure pulsations in the turbulent boundary layer was presented. The method was based on the subsequent application of the grid-based and mesh-free methods. The proposed approach was universal and can be used without any additional empirical or artificial data and allows to cut sharply computational cost compared to the DNS and LES methods. Nevertheless, several issues of the proposed method require detailed investigation and further development. The most important of them are:

- An estimation of the influence of the wall boundary condition on the simulation results;
- Investigation of the possibility of vortex-generators “enlargement” across cell’s groups to save computational resources and reduce simulation time;
- Investigation of the wave shed’s length influence on the pressure pulsations on the body;
- The detailed estimation of the discretization parameters, including a thorough investigation of the influence of time and space discretization, free vortices generation step and computational radius.

Author Contributions

V. Shabarov conceived the initial idea of the proposed method. P. Kalyasov chose the test problem and adapted the method to solve this problem. Pavel also conducted LES simulations. V. Shaposhnikov implemented the method as a computer program. F. Peplin conducted the simulations. The manuscript was written through the contribution of all authors. All authors discussed the results, reviewed, and approved the final version of the manuscript.

Conflict of Interest

The authors declared no potential conflicts of interest with respect to the research, authorship, and publication of this article.

Funding

The authors received no financial support for the research, authorship, and publication of this article.

References

[1] Martin, R., Soria M., Lehmkuhl O., Gorobets A., Canteand J., Vidal P., Noise Radiated by An Open Cavity At Low Mach Number, *Tenth International Conference on Computational Fluid Dynamics (ICCFD10)*, Barcelona, Spain, 2018.
[2] Yokoyama, H., Odawara, H., Iida A., Effects of freestream turbulence on cavity tone and sound source, *International Journal of Aerospace Engineering*, 2016, 7347106.
[3] Siefert, M. Ewert R., Sweeping sound generation in jets realized with a random particle-mesh method, *15th AIAA/CEAS Aeroacoustics Conference (30th AIAA Aeroacoustics Conference)*, 2009.
[4] Ewert, R., Appel C.,Dierke J., Herr M., RANS/CAA based prediction of NACA 0012 broadband trailing edge noise and experimental validation, *15th AIAA/CEAS Aeroacoustics Conference (30th AIAA Aeroacoustics Conference)*, 2009.
[5] Dergachev, S., Marchevsky I., Shcheglov G., Flow simulation around 3D bodies by using Lagrangian vortex loops method with boundary condition satisfaction with respect to tangential velocity components, *Aerospace Science and Technology*, 94, 2019, 105374.
[6] Wu, L., Jing X., Sun X., Prediction of vortex-shedding noise from the blunt trailing edge of a flat plate, *Journal of Sound and Vibration*, 408, 2017, 20-30.
[7] Mathey, F., Aerodynamic noise simulation of the flow past an airfoil trailing-edge using a hybrid zonal RANS-LES, *Computers & Fluids*, 37(7), 2008, 836-843.
[8] Ewert, R., Dierke, J., Siebert, J., Neifeld, A., Appel, C., Siefert, M., Kornow, O., CAA broadband noise prediction for aeroacoustic design, *Journal of Sound and Vibration*, 330(17), 2011, 4139-4160.
[9] Manninen, M., Taivassalo V., Kallio S., *On the mixture model for multiphase flow*, Technical Research Centre of Finland, Finland, 1996.
[10] Sheikholeslami, M., Abohamzeh, E., Jafaryar, M., Shafee, A., Babazadeh, H., CuO nanomaterial two-phase simulation within a tube with enhanced turbulator, *Powder Technology*, 373, 2020, 1-13.
[11] Sheikholeslami, M., Farshad, S. A., Shafee, A., Babazadeh, H., Performance of solar collector with turbulator involving nanomaterial turbulent regime, *Renewable Energy*, 163, 2020, 1222-1237.
[12] Sheikholeslami, M., Jafaryar, M., Said, Z., Alsabery, A. I., Babazadeh, H., Shafee, A., Modification for helical turbulator to augment heat transfer behavior of nanomaterial via numerical approach, *Applied Thermal Engineering*, 182, 2020, 115935.
[13] Buaria, D., Pumir A., Bodenschatz E., Self-attenuation of extreme events in Navier–Stokes turbulence, *Nature Communications*, 11(1), 2020, 1-7.
[14] Moreau, S., Christopher J., Roger M., LES of the trailing-edge flow and noise of a NACA0012 airfoil near stall, *Proceedings of the Summer Program*, 2008.
[15] Wang, M., Moreau, S., Iaccarino, G., Roger, M., LES prediction of wall-pressure fluctuations and noise of a low-speed airfoil, *International Journal of Aeroacoustics*, 8(3), 2009, 177-197.
[16] Wu, H., Moreau S., Sandberg R.D., On the noise generated by a controlled-diffusion aerofoil at Rec= 1.5× 105, *Journal of Sound and Vibration*, 487, 2020, 115620.
[17] Suvorov, A. S., Korotin, P. I., Sokov, E. M., Finite element method for simulating noise emission generated by inhomogeneities of bodies moving in a turbulent fluid flow, *Acoustical Physics*, 64(6), 2018, 778-788.
[18] Menter, F. Zonal two equation kw turbulence models for aerodynamic flows, *23rd Fluid Dynamics, Plasmadynamics and Lasers Conference*, 1993.
[19] Chipongo, K., Khiadani M., Lari K.S., Comparison and verification of turbulence Reynolds-averaged Navier–Stokes closures to model spatially varied flows, *Scientific Reports*, 10(1), 2020, 1-21.
[20] Loytsansky L.G., *Fluid Mechanics*, Gostekhizdat, Moscow, 1950.
[21] Menter, F.R., *Best practice: scale-resolving simulations in ANSYS CFD*. ANSYS Germany GmbH, 2012.
[22] Spalart, P.R., Strategies for turbulence modelling and simulations, *International Journal of Heat and Fluid Flow*, 21(3), 2000, 252-263.

ORCID iD

Vasiliy Shabarov https://orcid.org/0000-0003-4102-4642
Pavel Kalyasov https://orcid.org/0000-0003-2920-3226
Vitaliy Shaposhnikov https://orcid.org/0000-0003-2830-0710
Fedor Peplin https://orcid.org/0000-0001-8149-7992

How to cite this article: Shabarov V., Kalyasov P., Shaposhnikov V., Peplin F. Method of Unsteady Hydrodynamics Characteristics Determination in Turbulent Boundary Layer, *J. Appl. Comput. Mech.*, 7(2), 2021, 849–857. https://doi.org/10.22055/JACM.2020.34992.2534